

From colloidal aggregation to spinodal decomposition in sticky emulsions

P. Poulin^{1,2,a}, J. Bibette¹, and D.A. Weitz²

¹ Centre de Recherche Paul Pascal/CNRS, avenue A. Schweitzer, Pessac 33600, France

² Dept. of Physics and Astronomy, University of Pennsylvania, Philadelphia PA 19104, USA

Received: 7 April 1998 / Revised: 19 August 1998 / Accepted: 21 August 1998

Abstract. Aggregation mechanisms of emulsions at high initial volume fractions ($\phi_0 > 0.01$) is studied using light scattering. We use emulsion droplets which can be made unstable towards aggregation by a temperature quench. For deep quenches and $0.1 > \phi_0 > 0.01$, the aggregation mechanism is identified as diffusion-limited cluster aggregation (DLCA). An ordering of the clusters, which is reflected by a peak in the scattering intensity, is shown to result from the intercluster separation, exhibiting different scaling than that observed at lower volume fractions. This manifests an increasing similarity to spinodal decomposition observed as ϕ_0 is increased. For $\phi_0 > 0.1$ and shallow quenches, different mechanisms, closer to spinodal decomposition, are observed. These results allow the subtle boundaries between DLCA and spinodal decomposition to be explored.

PACS. 61.43.Hv Fractals; macroscopic aggregates (including diffusion-limited aggregates) – 82.70.Gg Gels and sols – 64.70.Ja Liquid-liquid transitions

Colloid aggregation is a coarsening process driven solely by kinetics; colloidal particles stick irreversibly to one another as they collide due to their diffusive motion. The resultant bonds can be sufficiently strong to prevent further rearrangement, leading to highly disordered and tenuous clusters, whose structure can be well-described as fractal [1]. If there is no repulsive barrier preventing clusters from sticking upon collision, the coarsening is driven solely by the diffusion-induced collisions between the growing clusters. This regime, called diffusion-limited cluster aggregation (DLCA), is amenable to detailed theoretical analysis, and has become an important base case on which we can build our understanding of other kinetic growth processes. The initial growth of the DLCA clusters is completely random; nevertheless, recent experiments with slightly more concentrated suspensions than previously studied, have shown that a surprising order can develop, manifested by a pronounced peak in the small angle scattering intensity as a function of wave vector, $I(q)$, which reflects the development of a characteristic length scale in the suspension [2,3]. While first observed in three-dimensional DLCA, similar behavior has also been reported for two-dimensional aggregation of particles on the surface of a fluid [4]. This surprising observation suggests that DLCA has much in common with a completely different coarsening process, spinodal decomposition, which is not driven exclusively by diffusion, but which instead reflects the evo-

lution of phase separation as the system is quenched away from equilibrium [5]. In both processes there is a pronounced peak in $I(q)$; in both processes this peak moves to smaller q as the system coarsens; in both processes, $I(q)$ exhibits scaling behavior [2,6–9]. At long times, DLCA must produce a gel which spans the system, preventing further coarsening. By contrast, spinodal decomposition must ultimately result in the complete separation of the two phases; however, recent studies of spinodal decomposition in colloidal systems [10] have shown that a deep quench can result in the formation of a gel-like structure, kinetically arresting the phase separation, and further enhancing the apparent similarity between the two coarsening processes. Despite the intriguing similarities in the two coarsening processes, there are intrinsic differences between DLCA and spinodal decomposition. In spinodal decomposition, the characteristic length scale is initially set by the fastest growth of a dominant fluctuation; by contrast, in DLCA, this length scale must originate solely from the diffusive motion of the particles. Thus, a complete understanding of their link remains elusive, calling for further exploration of their similarities.

In this work, we report the results of an experimental study of the inherent similarities between aggregation and spinodal decomposition. We focus on the behavior of colloid aggregation as the initial volume fraction of particles, ϕ_0 , is increased, and show that the similarity to spinodal decomposition becomes even more pronounced with increasing ϕ_0 . We use monodisperse emulsion droplets,

^a e-mail: poulin@crpp.u-bordeaux.fr

which can be made unstable towards aggregation by a temperature quench; this allows us to explore the DLCA process for suspensions with initial volume fractions above $\phi_0 = 0.01$. Index matching the suspensions enables us to probe their behavior with light scattering, even at these high volume fractions. We report the observation of three different scenarios for the aggregation; these are controlled by the quench depth and the initial volume fraction. Each of these scenarios bears a striking similarity to spinodal decomposition; together, they provide further important insight into the nature of this similarity. In the first case, when $0.008 < \phi_0 < 0.1$, a pronounced peak in $I(q)$ is observed at a scattering wave vector, q_m . This evolves with time as $q_m \sim t^{-1/3}$; this is in marked contrast to the behavior at lower ϕ_0 , where $q_m \sim t^{-1/d_f}$, with d_f the fractal dimension of the clusters. However, in both cases, all the light scattering data at later times can be scaled onto a single curve, with the scaling reflecting the fractal structure of the clusters. Thus, while the fractal dimension of the clusters controls all the scaling at low ϕ_0 , it is the dimension of space that controls the scaling of q_m with t for higher ϕ_0 , identical to the behavior observed for spinodal decomposition. In the second case, when $\phi_0 > 0.1$, completely different behavior is observed, and the similarity with spinodal decomposition becomes even more pronounced; we find that q_m remains constant in time, while $I(q_m)$ increases exponentially with t , similar to the behavior expected in the early stages of a spinodal decomposition within the linear Cahn-Hilliard theory [5,11]. However, full phase separation is arrested by gelation of the system. Finally, the third case highlights the merging of aggregation and spinodal decomposition. When the temperature quench is not as deep, and samples with a high ϕ_0 are used, no gelation is observed; instead we observe a process akin to a full phase separation in that the resultant clusters are highly compact and can not span the system to form a gel. Nevertheless, marked phase separation still occurs, as there are no remaining free particles in equilibrium with the clusters. These experimental results elucidate the nature of DLCA at higher volume fractions and further cement the intriguing analogy between aggregation and spinodal decomposition.

We use emulsions composed of monodisperse silicone oil droplets in water mixed with glycerol (30% by weight) to increase the index of refraction and eliminate multiple scattering, and with 2 mM sodium dodecyl sulfate to stabilize the droplets. The droplet radius is $a = 0.19 \mu\text{m}$, as determined with static light scattering. The suspension also contains 0.35 M NaCl which makes the droplets sticky as the temperature is lowered to the onset of the attractive interaction at 35 °C. Above 35 °C, there is no appreciable attractive interaction; between 34.7 °C and 35 °C, the attraction is weak, leading to an equilibrium between dilute and concentrated phases of droplets; below 34.7 °C the attraction is much greater than $k_B T$ [12], the thermal energy, and the droplets stick strongly to one another upon collision. This allows us to rapidly and controllably induce aggregation and then gelation of the emulsions. This is accomplished by holding the sample temperature

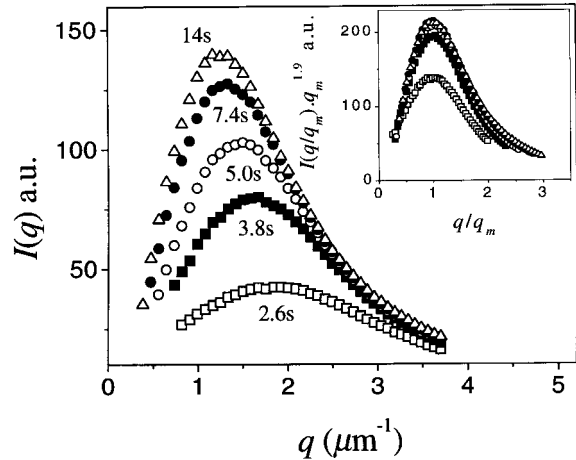


Fig. 1. Intensity as a function of scattering wave vector for an emulsion with $\phi_0 = 0.04$ at a series of times. The inset shows that, except at the earliest times, the data can be scaled onto a single curve.

above 45 °C, and then quenching the sample temperature to 30 °C, at rates of 3–5 °C/s. The evolution of the system structure is monitored by static light scattering. The sample is contained in a thin cell, 100 or 200 μm thick, and light from an Ar⁺ laser is passed through the cell. The scattered light is imaged onto a screen, which is in turn imaged onto a CCD camera. These images are digitized and the intensity as a function of scattering vector, $I(q)$, is determined as a function of time.

1 First scenario, $0.008 < \phi_0 < 0.1$ and deep quenches

Typical results for a sample which follows the first scenario of aggregation are shown in Figure 1. We plot a series of $I(q)$ taken at different times after the aggregation begins using a sample with an initial droplet volume fraction of $\phi_0 = 0.04$. We choose $t = 0$ as the time when the first perceptible change in the scattering intensity is observed. There is a pronounced peak in $I(q)$ which grows in intensity and moves to lower q with time; ultimately the system gels, and there are no further changes in $I(q)$. The scattering wave vector of the maximum intensity defines a characteristic length scale of the system, q_m^{-1} ; at gelation, we define this length scale as q_g^{-1} . As has been observed previously [2,4,8], after a brief initial stage, all the scattering curves can be scaled onto a master curve by plotting $q_m^{d_f} I(q/q_m)$ as a function of q/q_m . This scaling is illustrated in the inset of Figure 1, where we use $d_f = 1.9$. Similar behavior is observed for all concentrations studied below $\phi_0 = 0.08$, with values of d_f , required for the scaling, varying from 1.7 to 1.9.

The time evolution of q_m that we observe is markedly different than that observed at lower ϕ_0 . There, the peak in the scattering from aggregating colloids originates from conservation of mass [13]; each cluster is surrounded by a

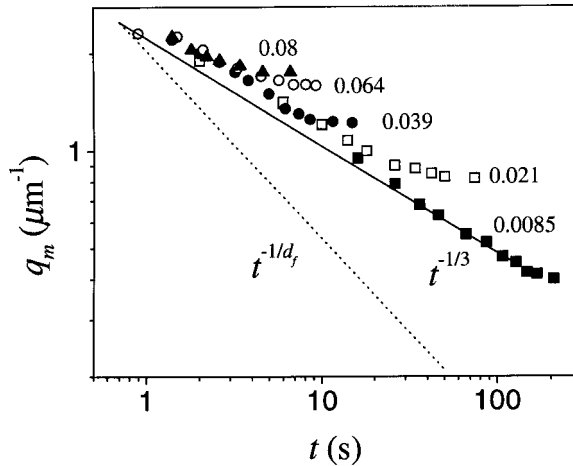


Fig. 2. The time evolution of the scattering wave vector of the maximum intensity, q_m , for data with several different ϕ_0 . All the data lie on a single curve, decreasing as $t^{-1/3}$.

depletion shell, with the resultant form factor of cluster plus depletion shell leading to the observed peak. Thus, $q_m^{-1} \sim R$, the characteristic size of the clusters, and the time evolution of q_m can be calculated from the condition of diffusion-limited growth, which gives the rate of change of the concentration of clusters, n [14],

$$\frac{dn}{dt} = -16\pi DRn^2 \quad (1)$$

where D is the cluster diffusion coefficient, and the product DR is a constant. The cluster concentration is determined from ϕ_0 by conservation of mass, assuming equal cluster size,

$$n = \frac{\phi_0}{48\pi a^3} \left(\frac{a}{R}\right)^{d_f}. \quad (2)$$

Integrating equation (1) using equation (2) gives, in the limit of long times, $q_m \sim (\phi_0 t)^{-1/d_f}$. The first experimental observation of this ring [2] using $\phi_0 < 10^{-4}$ indeed found $q_m \sim t^{-0.56}$, consistent with this prediction. By contrast, our data exhibit a completely different behavior, as shown in Figure 2, a logarithmic plot of q_m as a function of t for several different ϕ_0 . Unexpectedly, we find that $q_m \sim t^{-1/3}$ and that the data all scale onto a single curve, independent of ϕ_0 . Thus, the origin of the peak in the structure factor cannot be due to the characteristic size of the clusters; instead, the peak must reflect spatial ordering of the clusters, in addition to uniformity in size. To see this, we replace the condition for the cluster concentration, equation (2), by the condition that the clusters be equally spaced,

$$n = \frac{1}{6\pi d^3} \quad (3)$$

where d is the separation between the center of neighboring clusters. We consider $q_m \sim d^{-1}$ and we integrate equation (1) using equation (3) to obtain, at long times,

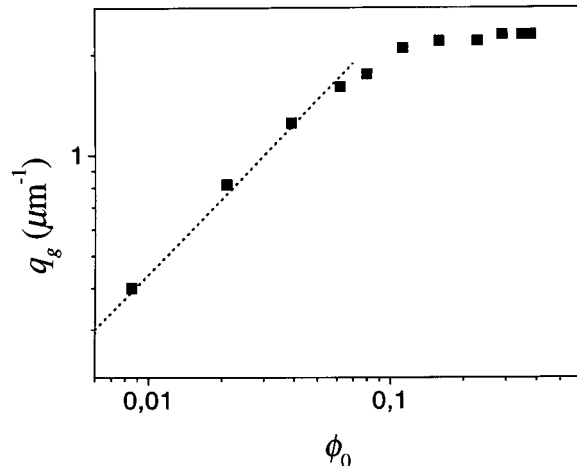


Fig. 3. The dependence of q_g on ϕ_0 . For $\phi_0 < 0.1$, the data have a $\phi_0^{0.75}$ dependence, consistent with DLCA clusters with a fractal dimension of $d_f = 1.7$.

$q_m \sim t^{-1/3}$, independent of ϕ_0 , exactly as observed. This same $t^{-1/3}$ scaling is also predicted and observed for spinodal decomposition [5]; thus the behavior of DLCA at the higher ϕ_0 investigated here is remarkably similar to that of spinodal decomposition. This must arise from the predominance of spatial correlations in the DLCA process; this is in sharp contrast to the behavior at very low ϕ_0 , where the peak arises from the depletion shell around the clusters [8, 13].

The behavior observed in our data is similar to that observed in recent simulations of DLCA which preserve the spatial configuration of the clusters [7, 15, 16]. In the simulations, a minimum in the density correlation function, $g(r)$, was observed, corresponding to the average cluster separation; its time evolution was described by a power law with an exponent closer to $1/3$ than to $1/d_f$. In fact, the exponent that best describes our data for $\phi_0 = 8.5 \times 10^{-3}$ is 0.36 ± 0.2 , in excellent agreement with the value observed in the simulations for a similar ϕ_0 . This value is slightly greater than $1/3$, presumably reflecting the trend towards larger values that must occur as ϕ_0 becomes very small and the exponent approaches $1/d_f$. We emphasize that analysis of $q_m(t)$ provides a unique way to obtain structural information in three-dimensional systems where direct observation is impossible. Interestingly, in two-dimensional systems, where direct imaging is possible, it was experimentally observed that the peak of the structure factor is linked to the separation between neighboring clusters rather than to the cluster size [4].

2 Second scenario, $0.1 < \phi_0 < 0.4$ and deep quenches

The similarity between the aggregation process of these sticky emulsions and spinodal decomposition is further buttressed by the behavior at high ϕ_0 , evidenced by the ordering at gelation, as determined by q_g . For diffusion

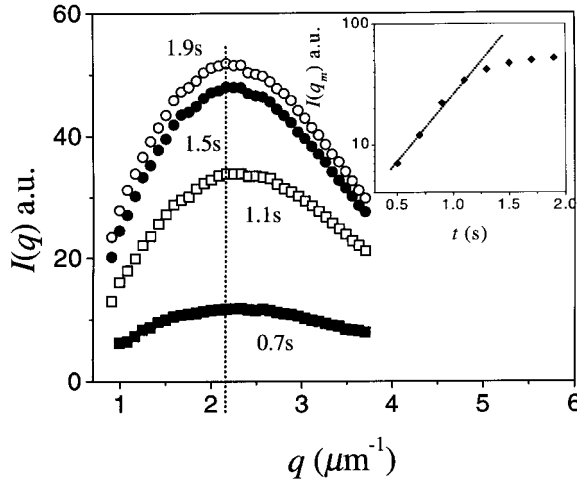


Fig. 4. Time evolution of $I(q)$ for $\phi_0 = 0.23$. The peak position does not change, while the intensity increases exponentially with time (inset).

controlled gelation, we expect $q_g \sim \phi_0^{1/(3-d_f)}$; this is observed, as shown by the dashed line in Figure 3, which is a fit to a power-law dependence of q_g on ϕ_0 for the data with $\phi_0 < 0.1$. The exponent is 0.75, close to the expected value, 0.83 for $d_f = 1.8$. However, for $\phi_0 > 0.1$, there is a sharp change, and very little variation of q_g with ϕ_0 is observed. There is still a pronounced peak in $I(q)$; however, q_m is independent of t , as shown in Figure 4 for $\phi_0 = 0.23$. Moreover, the intensity at q_m grows exponentially with time until gelation occurs, typically in less than 2 s; this is shown in the inset of Figure 4. Similar behavior is observed for all $\phi_0 > 0.1$, although the peak in $I(q)$ becomes broader as ϕ_0 is increased. This broadening is noticeably more pronounced when $\phi_0 > 0.3$. For $\phi_0 > 0.4$ no peak are longer observed. The behavior in this second scenario is similar to that expected for the early stages of a spinodal decomposition within the framework of the Cahn-Hilliard linear theory [5,11]. The origin of this behavior for these emulsions is not clear. This may be an intrinsic phenomenon, reflecting the inherent similarity of DLCA with spinodal decomposition for high ϕ_0 . Alternatively, this may be a consequence of the aggregation rate becoming comparable to the quench rate at these high volume fractions. Simulations at these high ϕ_0 would be most helpful in determining the intrinsic nature of the behavior of this second scenario.

3 Third scenario, $0.1 < \phi_0 < 0.4$ and shallow quenches

The possibility of the quench rate competing with the aggregation rate can be investigated further by performing deliberately weaker or slower quenches; this is the third scenario. This provides an opportunity for the structures to anneal, thereby achieving more uniform and higher density; the deviation from equilibrium is less extreme than any process that is completely kinetically controlled, such

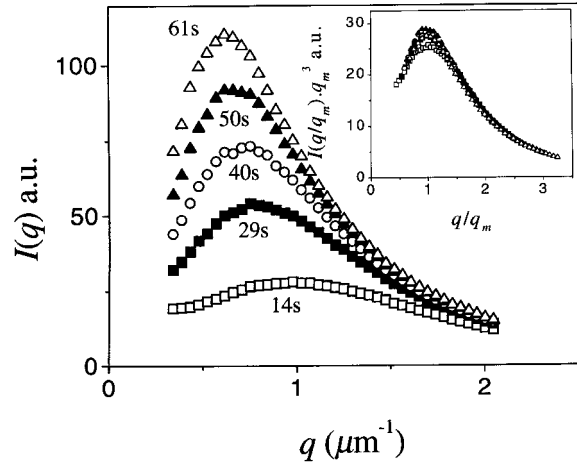


Fig. 5. The time dependence for an emulsion with $\phi_0 = 0.16$, weakly quenched so that it undergoes spinodal decomposition. The data scale (inset) but with an exponent of 3, indicative of compact, rather than fractal, clusters.

as pure cluster aggregation, and thus, this regime is even closer to spinodal decomposition. This scenario is achieved by quenching only ~ 0.3 °C below 35 °C where the interaction is weaker than at lower temperature [12]; here the attraction is still large enough to cause the particles to stick, but is not sufficient to prevent rearrangements after the particles have stuck. This leads to more “classical” phase separation rather than an aggregation process. A pronounced peak is observed in $I(q)$, as shown in Figure 5. The value of q_m decreases with time, and, as shown in the inset, scaling is again observed as in the first scenario; however this scaling is now accomplished by using $I(q/q_m)q_m^3$, exactly the same as for spinodal decomposition [5]. In this third scenario, the system can fully phase separate rather than gel, and q_m continues to decrease until it can no longer be observed.

The distinction between the deep quench, which is the second scenario, and the shallow quench, which is the third scenario, is in fact rather delicate. Small changes in the quench depth can result in large changes in the aggregation behavior. For example, a slightly deeper quench can result in the formation of a gel rather than a phase separation; however this gel has a q_g that is smaller than that observed for a very deep quench, reflecting the fact that rearrangements within the clusters makes them more compact so that they must be larger in order to form a gel. In fact, a previous study [3] of this behavior was plagued by this problem; the reported ϕ_0 dependence of q_g exhibited a deviation from power-law growth at $\phi_0 \sim 0.01$, presumably because the quench rate was not high enough. However, the weaker quench does illustrate another of the possible approaches of DLCA to spinodal decomposition. Moreover, it suggests that the behavior for $\phi_0 > 0.1$ does indeed correspond to spinodal decomposition.

The sticky emulsions studied here are an ideal system for investigating the analogy between aggregation and spinodal decomposition. Because the degree of adhesion is controlled by the magnitude of the temperature quench,

the behavior of these emulsions can be varied between spinodal decomposition with a shallow quench, and DLCA with a deep quench. However, even with a deep quench, the DLCA-like behavior becomes increasingly similar to that of spinodal decomposition as the initial volume fraction of the particles increases. This reflects the fragile boundary between these two important coarsening mechanisms; both processes engender ordering and scaling of the light scattering, and both processes engender scaling of their characteristic length scales, as signified by the time evolution of the wave vector of the peak of the scattering intensity. In fact, the behavior reported here suggests that DLCA is simply one limit of spinodal decomposition, that is achieved with a deep quench and a very low volume fraction of one of the separating phases. In the traditional picture for spinodal decomposition, the initial characteristic length scale is determined by the depth of the quench, and decreases with increasing quench depth [5]. Does this length scale become identical to the one that characterizes DLCA in the limit of very deep quenches? Based on the results presented here, this is certainly a likely scenario. However, further investigation of the similarity between DLCA and spinodal decomposition is required to unambiguously determine this.

We acknowledge NSF (DMR 96-31279) and NASA (NAG 3-1858) for partial support of this work.

References

1. R. Jullien, R. Botet, *Aggregation and Fractal Aggregates* (World Scientific, 1987).
2. M. Carpineti, M. Giglio, Phys. Rev. Lett. **68**, 3327 (1992).
3. J. Bibette, T.G. Mason, H. Gang, D.A. Weitz, Phys. Rev. Lett. **69**, 981 (1992).
4. D.J. Robinson, J.C. Earnshaw, Phys. Rev. Lett. **71**, 715 (1993).
5. J.M. Gunton, M. San Miguel, P.S. Sahni, in *Phase Transition and Critical Phenomena*, edited by J.L. Lebowitz (Academic Press, London, 1983), Vol. 8, p. 267.
6. A.E. Gonzalez, G. Ramirez-Santiago, Phys. Rev. Lett. **74**, 1238 (1995).
7. A. Hasmy, R. Jullien, J. Non-crystall. Sol. **186**, 342 (1995).
8. F. Sciortino, P. Tartaglia, Phys. Rev. Lett. **74**, 282 (1995).
9. T. Sintès, R. Toral, A. Chakrabarti, Phys. Rev. E **50**, R3330 (1994).
10. W.C. Poon, A.D. Pirie, P.N. Pusey, Faraday Discuss. **101**, 65 (1995).
11. J.W. Cahn, J.E. Hilliard, J. Chem. Phys. **28**, 258 (1958).
12. P. Poulin, J. Bibette, Phys. Rev. Lett. **79**, 3290 (1997).
13. M. Carpineti, M. Giglio, V. Degiorgio, Phys. Rev. E **51**, 590 (1995).
14. E.D. Siggia, Phys. Rev. A **20**, 595 (1979).
15. A.E. Gonzalez, G. Ramirez-Santiago, Phys. Rev. Lett. **74**, 1238 (1995).
16. A.E. Gonzalez, G. Ramirez-Santiago, J. Coll. Interf. Sci. **182**, 254 (1996).